4-2009

Characterization of electrochemically grafted molecular layers on silicon for electronic device applications

Adina Scott
Purdue University - Main Campus, scott26@purdue.edu

David B. Janes
Purdue University, david.b.janes.1@purdue.edu

Characterization of electrochemically grafted molecular layers on silicon for electronic device applications

Adina Scott[a)] and David B. Janes
School of Electrical and Computer Engineering, Birck Nanotechnology Center, Purdue University, West Lafayette, Indiana 47907, USA

(Received 20 November 2008; accepted 18 February 2009; published online 6 April 2009)

Recently, there has been considerable interest in developing organically functionalized silicon surfaces for a variety of applications including sensing and nanoelectronics. In this study, a series of as-deposited, *para*-substituted aryl-diazonium molecular layers covalently grafted to ⟨111⟩-orientation silicon are characterized using a variety of surface analysis techniques. Collectively, these measurements suggest that relatively ideal molecular layers can be achieved with a variety of headgroups. Submonolayer amounts of silicon oxide are detected on all modified surfaces and the extent of silicon oxidation depends on the molecular substituent. For electronic device applications, it is necessary to apply contacts to molecular layers while maintaining their structural and chemical integrity. To this end, *in situ* spectroscopies are used to infer the effects of metallization on such molecular layers. It is found that applying gold using a soft evaporation technique does not significantly perturb the molecular layer, whereas the application of copper using the same technique induces changes in the molecular vibrational spectra. Two complementary *in situ* spectroscopic methods are analyzed to more accurately determine the chemical properties of gold/molecule/silicon junctions. The physical mechanisms of the measurements and consequences for interpretation of the resulting spectra are discussed. © *2009 American Institute of Physics*. [DOI: 10.1063/1.3103337]

I. INTRODUCTION

Modified semiconductor surfaces are are great interest due to their potential application in nanoelectronics, sensing, and biological applications.[1] Functionalized silicon is particularly relevant because of its ubiquitous use in integrated circuit technology. Covalent modification of Si through Si–C bonds is particularly attractive due to its robustness and flexibility. The isolated Si–C bond strength is 451 kcal/mol. The bond strength of the as-deposited molecules is likely different, but it is still very strong. It has been shown that Si surfaces modified with hydrocarbons are resistant to oxidation, even after boiling in solvents and exposure to hydrofluoric acid.[2] Molecular layers have been used as electrode passivation materials for Si electrodes for electrochemical applications.[3] The thermal stability for a few molecular species has been assessed and alkyl molecular layers on Si have been demonstrated to survive to temperatures of 300 °C.[4]

Chemical modification of silicon can be achieved by a number of derivitization methods which involve covalently attaching the molecular modifiers via stable Si–C bonds.[5,6] Most reported methods consider the attachment of aliphatic chains to ⟨111⟩ Si, which has been demonstrated by thermal,[7,8] radical,[9,10] electrochemical,[11] and radiation-assisted[12] methods. For molecular electronic applications, it is desirable to utilize molecular layers with extended conjugation because they have potentially higher conductivity and increased electronic functionality.[13] Functionalization of ⟨111⟩ Si with aromatic species has been demonstrated by electrochemical[14] and spontaneous[15,16] reduction of aryl-diazonium salts. Electrochemical reduction of *para*-substituted aryl-diazonium salts can be carried out rapidly in ambient laboratory conditions for a variety of molecular species using dry solvent or acidic aqueous solutions, yielding densely packed molecular layers.[2,17]

A number of characterization techniques can be used to evaluate the molecular layers on surfaces.[6,18–20] Collectively, these techniques can provide information about the presence of the molecular species, approximate surface coverage, thickness and bonding characteristics, as well as chemical modifications which may have occurred during deposition. A few electrochemically grafted aryl molecular layers on silicon and carbon have been studied using Rutherford backscattering spectroscopy, electrochemical methods, scanning tunneling microscopy, atomic force microscopy (AFM), and x-ray photoemission spectroscopy (XPS).[2,21–23] It is found that the density and thickness of the molecular layer are functions of grafting conditions and molecular substituent, indicating that careful characterization and control of grafting potential and charge can lead to well-defined molecular layer structure. It has been demonstrated by infrared spectroscopy that the addition of an *in situ* etchant to aqueous solutions suppresses oxidation of the silicon surface during molecular grafting.[24] Applications such as electronic devices typically require a dense molecular layer as well as application of a top contact such as an evaporated metallic layer. Electrical measurements such as current-voltage or capacitance-voltage show systematic trends based on the molecular species that is employed[25–27] which provide indirect evidence of the integrity of the molecular layers within the

[a)]Electronic addresses: scott26@purdue.edu.

device structures. However, it is also important to study the structural/chemical characteristics of the molecular layers following metallization, since the deposition process can have significant effects on the molecular layer.[28–30] Recently, several *in situ* characterization techniques, i.e., techniques which allow characterization of the molecular layer following metallization, have been employed to study metal/molecule/silicon structures.[31,32]

In this study, the electrochemical reduction technique is used to deposit molecular layers of several species on silicon surfaces. The as-deposited molecular layers are studied using a variety of surface analysis techniques. Two complimentary *in situ* techniques are used to evaluate the influence of metal deposition on a molecular layer. Collectively, these measurements are used to assess the chemical and structural properties of the molecular layers.

II. SAMPLE PREPARATION

A. Hydrogen passivation

Hydrogen-terminated ⟨111⟩ Si was prepared by wet etching.[33,34] *n*-type (P-doped, $N_d=3\times10^{15}$ cm^{-3}), *n*-type double side polished (As-doped, $N_d=3\times10^{15}$ cm^{-3}), and *p*-type (B-doped $N_a=4\times10^{19}$ cm^{-3}) silicon wafers were used in this study. The wafers were coated with photoresist to protect the surface from mechanical damage and diced using a dicing saw. The photoresist was removed from the wafer pieces by soaking them in acetone. The Si pieces were cleaned by sonicating them for 5 min in toluene, 5 min in acetone, and 5 min in methanol. This sequence was then repeated to ensure that the particulate contamination from the dicing process was removed. The samples were then cleaned by immersion in hot piranha solution (either 1:1 volume ratio H_2SO_4:H_2O_2 or Nanostrip 2X) for 15–20 min to remove any residual organic contamination. The samples were removed from the piranha solution and rinsed repeatedly in ultrapure water. Hydrogen termination was achieved by etching the freshly cleaned samples for 12 min in concentrated aqueous ammonium fluoride solution which had been degassed by bubbling with nitrogen for at least 30 min in a teflon beaker.[35] The samples were then rinsed briefly with ultrapure water which had been degassed by bubbling with nitrogen and were dried under a stream of nitrogen. It has been reported that similarly prepared surfaces are stable for a period of hours under ambient conditions, exhibiting only submonolayer coverage of silicon oxide after 24 h in air.[36] In this study, all characterization and processing of these surfaces was initiated within 30 min of hydrogen terminating the samples.

B. Molecular grafting

Silicon surfaces modified by substituted aryl species were prepared by electrochemical reduction of *para*-substituted aryl-diazonium salts in an aqueous, acidic solution.[14,17,37] Bromobenzenediazonium tetrafluoroborate (B-benz), diethylanilinebenzenediazonium tetrafluoroborate (D-benz), methoxybenzenediazonium tetrafluoroborate (M-benz), nitrobenzenediazonium tetrafluoroborate (N-benz), 2-methyl 4-nitrobenzenediazonium tetrafluoroborate (2M 4N-benz), and 2-methoxy 4-nitrobenzenediazonium tetrafluoroborate (2MO 4N-benz) were purchased from Sigma Aldrich and used without further purification. A custom three-electrode electrochemical cell with a Pt mesh counter-electrode, Au wire pseudoreference electrode, and the freshly hydrogen-terminated silicon sample as the working electrode was used for molecular deposition. An Ohmic contact was made to the silicon by applying InGa eutectic and the sample was mounted on a sample holder with a Cu contact. A solution of 1:1:250 H_2SO_4:HF:ultrapure water by volume was prepared and degassed by bubbling with nitrogen for at least 20 min. 50 ml of this solution was added to a nitrogen-purged teflon electrochemical cell. A quantity of the desired molecular species adequate to form a 5 mM molecular concentration when dissolved in the solution was dissolved in a small quantity of deoxygenated de-ionized water and added to the cell just prior to application of a potential. Initial experiments were performed to determine the optimal grafting potential for each combination of molecular species and substrate type using cyclic voltammetry, the peak corresponding to the reduction of the diazo group was located, and this potential was selected as the optimal grafting condition. Molecular layer grafting for all samples was performed in a constant potential configuration while the current was monitored. The grafting potentials used in this study varied from −0.7 to −1.2 V (versus Au pseudoreference electrode) depending on the molecular species and substrate doping. During monolayer formation, the current drops exponentially. After monolayer coverage has been achieved, the current begins to drop linearly, corresponding to multilayer growth.[21] The reaction is stopped by switching the potential to zero as soon as the linear region of the grafting curve is encountered. Using this method, approximate monolayer coverage is achieved. The as-grafted species used in this study are shown in Fig. 1.

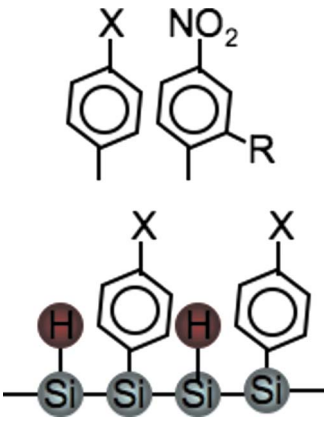

FIG. 1. (Color online) Molecules used in this study. X=Br (B- benz), $N(C_2H_5)_2$ (D-benz), OCH_3 (M-benz), NO_2 (N-benz), R=CH_3 (2M 4N-benz), R=OCH_3 (2MO 4N-benz). The ideal surface bonding is shown schematically.

After molecular layer deposition, the samples were cleaned by rinsing in de-ionized water followed by drying under a stream of nitrogen. They were then sonicated for 5 min in acetonitrile to remove physisorbed species and reaction by-products. The sonication step was repeated in fresh solvent and the samples were dried under a stream of nitro-

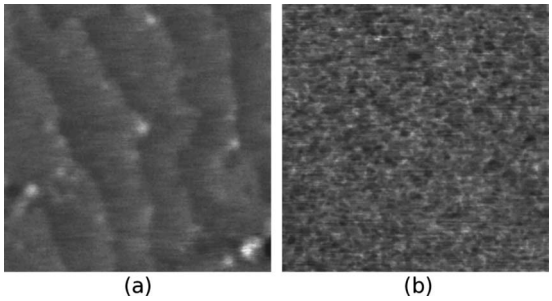

FIG. 2. 1×1 μm^2 AFM images of lightly doped (a) and heavily doped (b) hydrogen-terminated silicon wafers. The steps in (a) correspond to individual planes of Si atoms. The root-mean-square roughnesses of the images are 1.1 and 1.6 Å, respectively.

gen. At this stage, molecular layers are designated "as deposited." Samples were either transferred immediately to the measurement apparatus or stored in a drybox with continuous nitrogen purge until characterization was performed.

C. Metallization

In order to assess the influence of metal deposition on molecular layer characteristics, some samples were metallized by "soft" vapor deposition of gold or copper.[25,38,39] The samples are introduced into the chamber of a thermal evaporator with the sample surface oriented away from the metal source. The chamber is pumped down to a base pressure of at least 10^{-6} Torr. The chamber is then backfilled with argon to atmospheric pressure. This pump-purge cycle is repeated. The chamber is then pumped down to 6 mTorr and the evaporation is performed. During the metal deposition, the evaporation rate is monitored and restricted to a rate of 0.1 Å/s. The first 15–20 nm of metal is deposited using this procedure. The sample is then transferred to a standard electron-beam evaporator and an additional 150–200 nm of metal is deposited at a rate of 1 Å/s to enable further processing.

III. CHARACTERIZATION OF AS-DEPOSITED MOLECULAR LAYERS

Freshly prepared as-grafted molecular layers on silicon were analyzed using a number of standard surface characterization techniques to determine the structural and chemical properties of the surfaces.

A. AFM

AFM was performed using a Dimension 3100 atomic force microscope in cleanroom conditions to determine the topography of the samples. All scans were taken in contact mode with a silicon nitride AFM tip. Tapping-mode measurements were also performed and yielded similar results. All scans are 1×1 μm. n (P-doped) and $p+$ hydrogen-terminated silicon surfaces are shown in Fig. 2. For the lightly doped sample, steps are clearly visible on the surface. Each step is a large ⟨111⟩ facet of the crystal, with the edges corresponding to the height difference between individual planes of silicon atoms. The step height as measured by AFM is 2.2 ± 0.2 Å, which is in reasonable agreement with the atomic spacing for ⟨111⟩ silicon planes. For the heavily doped samples, step edges are not present, however, the surfaces are still very flat.

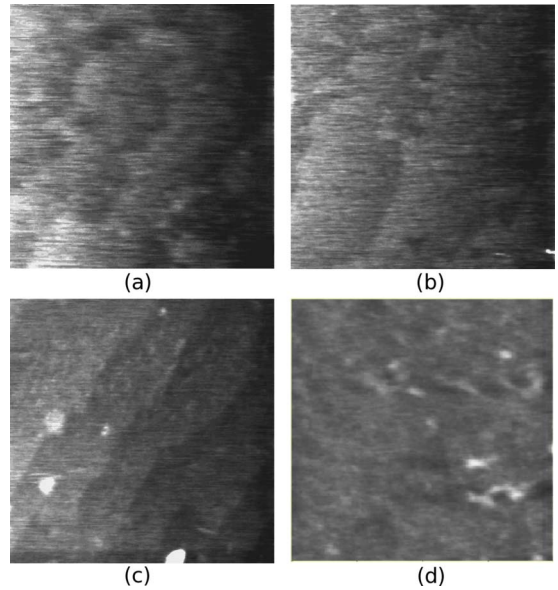

FIG. 3. (Color online) AFM images of B-benz (a), D-benz (b), M-benz (c), and N-benz (d) on n-type Si. Atomic step edges are still visible in (a)–(c), whereas (d) exhibits much less-ideal topography.

AFM images of the as-modified surfaces on n-type silicon are shown in Fig. 3. For B-benz, D-benz, and M-benz, the step edges are still clearly visible, indicating that the surface modification has not significantly affected the topography. This is consistent with the expected morphology of ideally modified surfaces. The N-benz surface no longer has clear step-edge structure, indicating that the molecular layer is sufficiently disordered to affect the surface topography.

B. XPS

XPS was performed using a Kratos Ultra DLD XPS system with monochromatic Al $K\alpha$ radiation ($h\nu=1486.6$ eV) and an analyzer pass energy of 20 eV. Spectra were obtained at normal incidence and angle resolved measurements were performed at 15° increments. Background subtraction and peak fitting were performed using CASAXPS software[40] with Gaussian–Lorentzian line shapes and linear or Shirley background subtraction. Wide scans were used to determine the species present on the surface. High-resolution scans were then performed in the regions where elements of interest were present to more precisely determine the atomic concentrations and oxidation states of those species. Angle-resolved XPS was utilized to determine the thickness and orientation of the various atomic species on the surface. Peak assignments were made based on comparing the binding energies with reports in the literature for similar molecular species.[41] All data shown were obtained on n-type Si; however, other substrate dopings were measured for a subset of the molecular species and showed similar results.

Survey scans of H-terminated and molecularly modified samples are shown in Fig. 4. For the H-terminated spectrum, the results are consistent with the presence of silicon with some hydrocarbon contamination and a small amount of

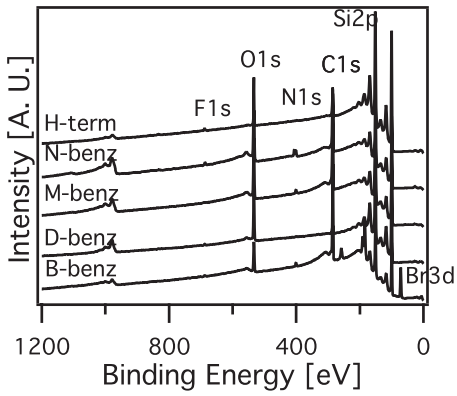

FIG. 4. XPS survey spectra of hydrogen-terminated and representative molecular samples. All spectra are shown in arbitrary units (A.U.).

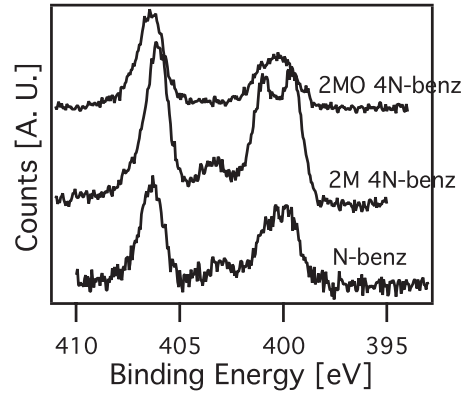

FIG. 6. N 1*s* spectra of nitro-substituted molecular layers. The peak near 407 eV is attributed to NO_2. The peaks in the vicinity of 400 eV are attributed to NH_x species which are formed by reduction of the nitro headgroup.

fluorine. The hydrocarbon is attributed to contamination from exposure of the samples to ambient as they are transported from the fume hood to the XPS system. The presence of fluorine can be attributed to the presence of a small amount of residual etchant on the surface or fluorinated hydrocarbon contamination from the teflon beakers used for etching. For the modified Si samples, the survey spectra show evidence of the silicon substrate, atomic species consistent with the adsorbate of interest, and residual hydrocarbon contamination. The absence of sulfur and boron on the surface confirms that the postdeposition cleaning removes the deposition solution and reaction by-products. High-resolution and angle-resolved XPSs were then performed to gain a more detailed understanding of the molecular layer composition and structure.

It has been shown that bromine-functionalized molecular layers can form various surface species due to molecular decomposition and interaction between the silicon and bromine.[18] High-resolution XPS of the Br 3*d* region of B-benz is shown in Fig. 5. The characteristic doublet due to the carbon-bound bromine is clearly visible. If silicon-bound bromine was present, there would be an additional doublet shifted to lower binding energy. The absence of these peaks indicates that electrochemical deposition does not decompose the aryl-bromine species. Angle-resolved XPS measurements indicate that the bromine is located at the sample surface which is consistent with the expected molecular layer orientation.

High-resolution spectra of the N 1*s* region for nitro-substituted species are shown in Fig. 6. There are peaks corresponding to multiple oxidation states of nitrogen which are attributed to various NO_x and NH_x species. The presence of these peaks suggests that the molecular headgroup is unstable and prone to reduction. There are two possible mechanisms for this: since the molecular grafting takes place at a reduction potential, it is possible that the nitro headgroup is reduced during molecular grafting. Alternately, the headgroup could spontaneously reduce after the molecular layer is put on the surface. NO_2 is quite unstable, and assuming

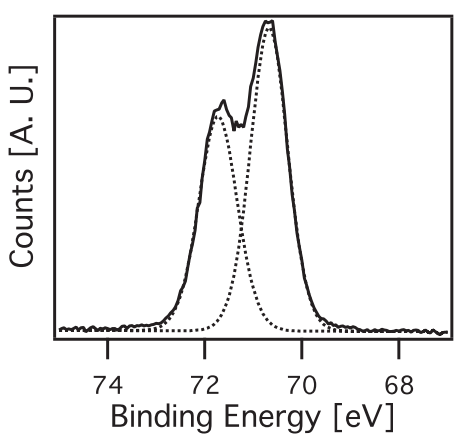

FIG. 5. Br 3*d* high-resolution XPS of Br 3*d* region of B-benz sample showing characteristic doublet consistent with carbon-bound bromine.

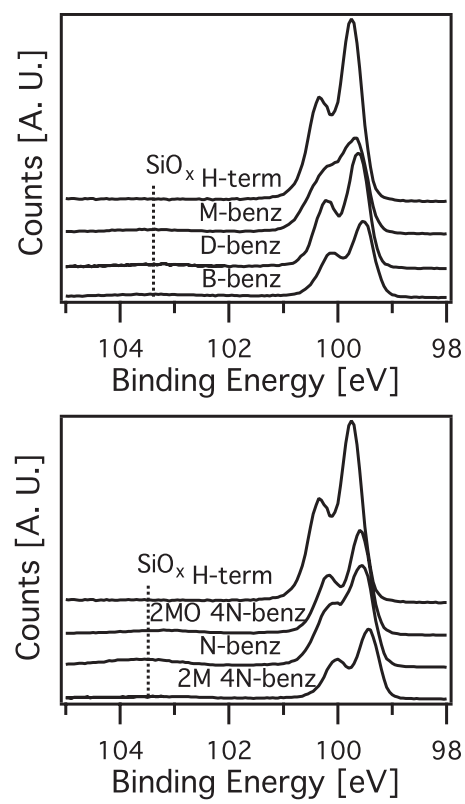

FIG. 7. High-resolution XPS of the Si 2*p* region for hydrogen-terminated and molecular samples.

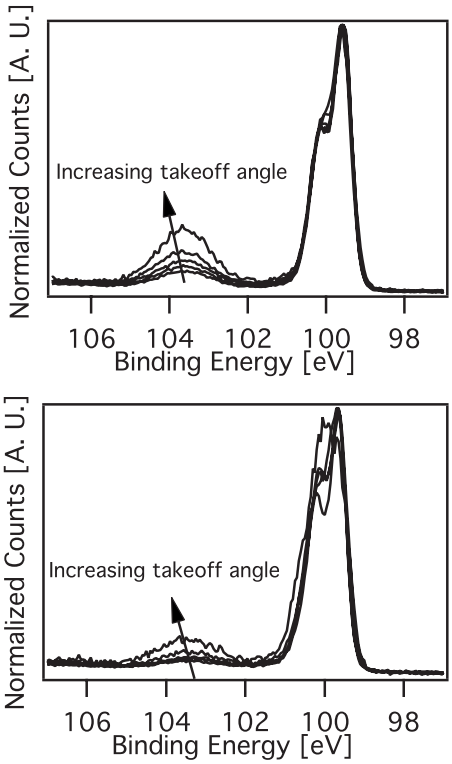

FIG. 8. Angle-resolved XPS of Si 2*p* region for molecular layers exhibiting high and low degrees of substrate oxidation. The takeoff angle was varied from 0° to 75°.

that some of the sites on the Si surface maintain the hydrogen termination, there is adequate hydrogen to react with. Angle-resolved XPS of the N 1*s* peak suggests that the nitrogen is primarily located at the sample surface, which is consistent with the molecules orienting in the expected manner.

The Si 2*p* region of the spectrum was analyzed in detail to characterize the level of oxide formation at the silicon surface. High-resolution scans at normal incidence for hydrogen-terminated and representative molecular samples are shown in Fig. 7. The characteristic doublet due to the Si 2*p* 3/2 and Si 2*p* 1/2 states is clearly visible. The silicon oxide peak is located at 103.5 eV. There is no distinguishable peak in this region for the hydrogen-terminated sample which is consistent with relatively ideal termination. The N-benz sample exhibits a fairly substantial oxide peak, whereas the M-benz sample has a very weak peak. It is found that the molecular headgroup affects the degree of substrate oxidation. In order to quantify this effect, angle-resolved XPS was used to offer a more quantitative determination of the degree of substrate oxidation. The amount of oxide was estimated by using a uniform overlayer model,[42] which is likely to overestimate the degree of oxidation because it fails to take into account the attenuation of the signal due to the molecular overlayer. High-resolution angle-resolved XPSs of samples exhibiting low and high degrees of surface oxidation are shown in Figs. 8(a) and 8(b), respectively. The oxide appears to form a partial monolayer since the experimentally determined thicknesses are less than 2.7 Å, which is the thickness of a SiO_x monolayer.[43,44] The calculated quantity of silicon oxide on the sample surfaces is given in Table I.

TABLE I. Quantity of silicon oxide for various molecular layers as calculated from Si 2*p* XPS peaks.

Molecular species	Amount of oxide (% of a monolayer)
B-benz	14
D-benz	12
M-benz	18
N-benz	80
2M 4N-benz	45
2MO 4N-benz	33

The hydrogen-terminated samples do not yield a measurable peak in the SiO_x region at any angle. The NO_2-containing layers exhibit a much higher level of oxidation than the other molecular samples. This supports the idea that the NO_2 may be reducing by taking the interstitial hydrogen from the Si surface.

High-resolution spectra of the C 1*s* regions of the hydrogen-terminated control sample and various molecular samples are shown in Fig. 9. The hydrogen-terminated sample has some hydrocarbon contamination with C–C, C–O, and O=C–OH species. All of the molecular samples have increased peak intensity in the C 1*s* region. In the case of M-benz and 2MO 4N-benz, there is a clear contribution near 287 eV due to the methoxy substituents. In order to accurately determine the molecular contribution to the carbon signal of the modified surfaces, it is necessary to correct for the presence of the hydrocarbon contamination.[19] Each spectrum is fitted using multiple Gaussian peaks. Assuming that the adsorbed hydrocarbon contamination on the molecu-

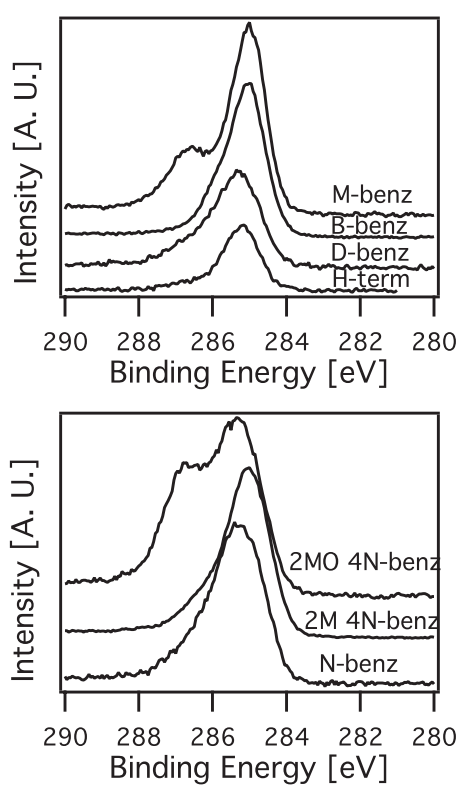

FIG. 9. As-measured high-resolution XPS of the C 1*s* region for hydrogen-terminated and molecular samples.

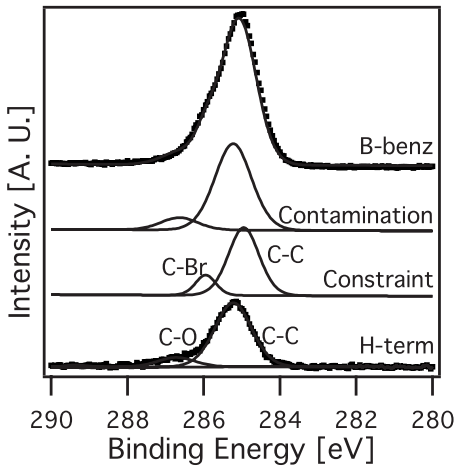

FIG. 10. Spectra illustrating the contamination correction procedure. The dots are measured spectra and solid lines are fits. The two peaks labeled "contamination" are attributed to hydrocarbon, while the two other peaks are attributed to C–C and C–Br species.

lar samples is similar to the hydrocarbon on the hydrogen-terminated sample, the fitted peaks can be attributed to carbon in the molecular layer or contamination based on comparison with the hydrogen-terminated sample C 1*s* spectrum, as shown in Fig. 10. The constraints obtained after correcting for the hydrocarbon contamination are shown in Fig. 11. In the case of D-benz, N-benz, and 2M 4N-benz, only one peak is resolved after this correction, which is consistent with previously observed XPS for similar compounds.[45,46] The peaks are located near 285 eV, which is consistent with aromatic carbon. The D-benz peak is shifted

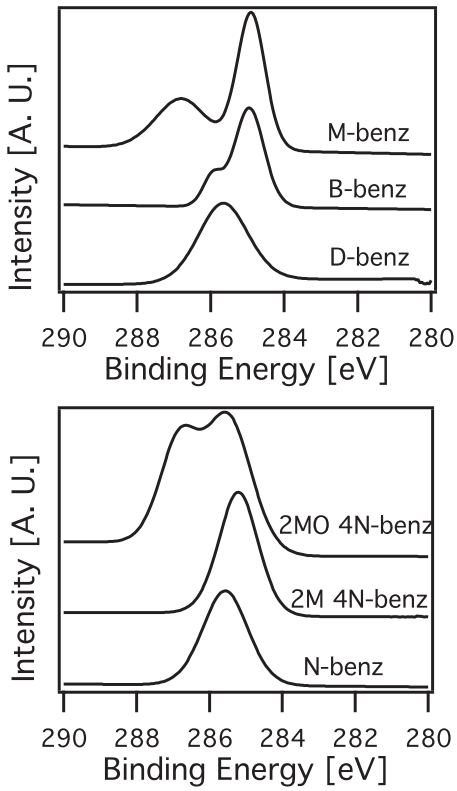

FIG. 11. XPS of the C 1*s* region for molecular samples corrected to remove contribution from hydrocarbon contamination.

TABLE II. Calculated and ellipsometrically measured thicknesses of molecular layers

Molecular species	Expected thickness (Å)	Measured thickness (Å)
B-benz	6.6	9.5 ± 1
D-benz	6.72	10.7 ± 1
M-benz	6.91	12.4 ± 1
N-benz	7.09	9.5 ± 1

to a relatively higher binding energy. The reason for this is under investigation. For B-benz, peaks corresponding to aromatic and Br-bound carbon are clearly visible. The M-benz and 2MO 4N-benz constraints each exhibits two peaks which can be attributed to aromatic carbon and oxygen-bound carbon from the methoxy substituent.

XPS measurements confirmed that chemical composition consistent with the expected adsorbates and some hydrocarbon contamination were present on all sample surfaces. Analysis of the Si 2*p* region revealed submonolayer quantities of silicon oxidation that is molecular-layer dependent with NO_2-substituted samples exhibiting relatively higher quantities of silicon oxide. Close analysis of the C 1*s* region including correction for hydrocarbon contamination revealed characteristics consistent with aromatic hydrocarbon and showed evidence for the methoxy substituent for M-benz and 2MO 4N-benz. High-resolution spectra of the N 1*s* regions of the NO_2-substituted species reveal the presence of NH_x species in addition to the expected NO_2 oxidation states. The Br 3*d* region for B-benz reveals that the molecular layer binds to the substrate in the expected orientation.

C. Ellipsometry

Ellipsometry was performed using a Gaertner Scientific L116S variable-angle Stokes ellipsometer with a $\lambda = 543.5$ nm light source. Measurements were performed on at least five regions on each sample of as-deposited molecular layers on *n*-type Si. The thickness was determined using a standard three-layer model. The molecular layer was considered using $n = 1.48$ and $k = 0$. Reference samples of hydrogen-terminated silicon and oxidized silicon were measured for comparison. It is difficult to accurately determine the thickness of very thin films with ellipsometry and the absolute height obtained is very sensitive to the optical parameters and other factors such as surface roughness. As such, trends in the data are considered, but the absolute film thicknesses as determined by this method are likely inaccurate. The expected molecular lengths as calculated by density functional theory and thicknesses of the molecular layers as extracted from ellipsometric measurements are given in Table II. The relative thickness of M-benz is larger than the other molecular layers which may indicate partial multilayer formation. The results are generally consistent with approximately one monolayer coverage for most samples.

D. Infrared spectroscopy

Fourier transform infrared (FTIR) spectroscopy was performed in a thermo-Nicolet spectrometer with a nitrogen-

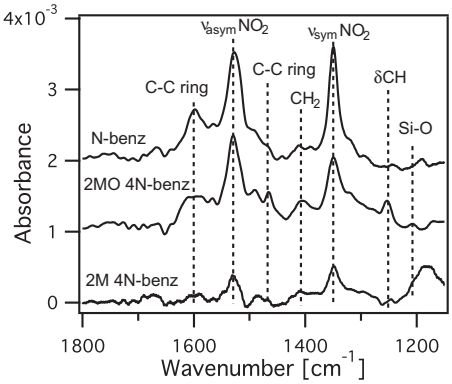

FIG. 12. Transmission infrared spectra of N-benz, 2M 4N-benz, and 2MO 4N-benz.

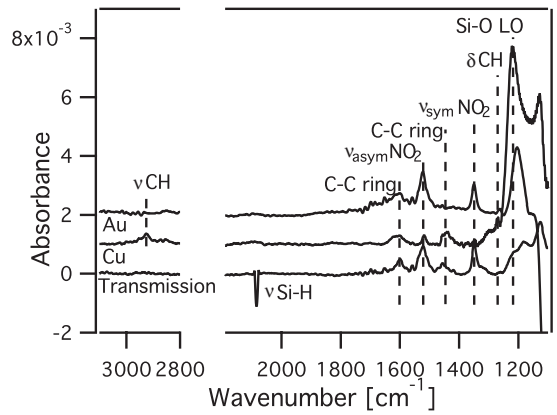

FIG. 13. Infrared spectra of as deposited (transmission) and metallized N-benz on Si. Cu significantly alters the molecular spectrum, whereas molecular features are preserved after Au deposition.

purged measurement chamber. Transmission FTIR was performed on *n*-type double-polished Si samples using *p*-polarized light incident at the silicon Brewster angle. The spectrum of a hydrogen-terminated Si sample is used as a background and subtracted from the spectrum of a functionalized silicon sample, yielding spectra which should be dominated by features of the adsorbate. Peaks were assigned based on comparison with values in the literature for similar molecular species. Peak fits were performed using Gaussian or Lorentzian peak shapes with IGORPRO. The absorption signal for a particular mode in infrared spectroscopy is related to the number of bonds present, their orientation relative to the surface, and the dipolar nature of the bond. Due to the small amount of adsorbate present in a molecular monolayer, only species with strongly dipolar bonds yielded spectra with clear molecular peaks. For this reason, only nitro-substituted molecular species will be considered in this section. FTIR of N-benz, 2M 4N-benz, and 2MO 4N-benz are shown in Fig. 12. The symmetric and asymmetric $(\nu_{\mathrm{sym}}, \nu_{\mathrm{asym}})$ NO_2 stretches are clearly visible at 1350 and 1540 cm^{-1}, respectively.[47–49] A C–C ring mode is evident near 1600 cm^{-1} for all samples. The amplitude of these modes is much lower for the 2M 4N-benz spectrum than the others, indicating that this molecular layer is less densely packed or ordered differently. For the 2MO 4N-benz sample, some additional C–C and CH ring modes are evident, likely due to enhancement from the methoxy substituent. The Si–O optical phonon mode can be located between 1200 and 1250 cm^{-1} depending on the thickness, composition, and ordering of the oxide. In all samples, there is a very weak mode in the low energy portion of this region indicating that there are trace amounts of disordered, nonstoichiometric oxide present.

IV. CHARACTERIZATION OF METALLIZED MOLECULES

The application of molecular layers to electronic devices often requires postprocessing such as the deposition of metal overlayers. It has been shown that such processing can drastically affect the structural and chemical integrity of the molecular layers.[50] As such, it is critical to develop and utilize *in situ* spectroscopic methods to probe metallized molecular layers and completed device structures. It is evident from Sec. III that applying multiple techniques for characterization of such layers is desirable because different methods offer different informations about the molecular layer structural and chemical properties. Using multiple characterization methods also allows for correlation of results, thereby increasing certainty in the interpretation of the results.

A. *p*-polarized back side absorption infrared spectroscopy

After metallization by soft evaporation of gold or copper, infrared spectroscopy was performed using an *in situ* back side technique using a thermo-Nicolet spectrometer with a Pike technologies reflection module.[51] After metallization, the sample back sides were cleaned by UV-ozone cleaning and etching to remove the molecular adsorbate, which would interfere with measurement of the metal/molecule/silicon junction properties. Infrared radiation is introduced through the back of the sample at the Brewster angle of silicon, travels through the silicon substrate to the metal-molecule interface where it interacts with the molecular layer, reflects off the metal, and travels back through the silicon substrate to the detector.[32,52] Peak collection and analysis were performed using the methods described in Sec. III D. Results for N-benz are shown in Fig. 13. Modes related to the benzene ring and NO_2 headgroup are clearly visible in the transmission spectrum. After deposition of gold by soft evaporation, the molecular signal is largely unchanged. A modest peak arises near 1200 cm^{-1} which is attributed to a small amount of disordered, nonstoichiometric silicon oxide, but otherwise the molecular layer appears unperturbed.[51] This is in contrast to prior results involving direct evaporation of Au at room temperature, which exhibited significant degradation of the *p*-polarized back side absorption infrared spectroscopy (pb-RAIRS) signal.[51] Deposition of copper by soft evaporation significantly attenuates the amplitudes of modes related to the nitro headgroup. A phonon mode consistent with significant oxidation of the silicon surface arises near 1230 cm^{-1}. Modes at 1250 and 2960, which are indicative of molecular decomposition and methyl formation, are also present. Collectively, these suggest that copper deposition perturbs the molecular layer. In contrast, metallization by soft evaporation of gold induces little

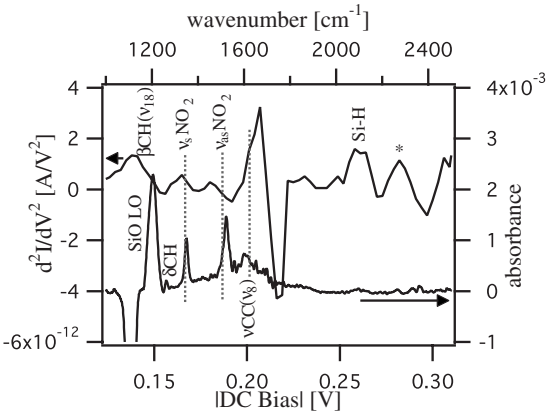

FIG. 14. Comparison of infrared and inelastic electron tunneling spectroscopies of Au/N-benz/Si structures.

change in the vibrational spectrum of the N-benz, indicating that soft gold is a promising electrode material for molecular electronic devices.

B. Inelastic electron tunneling spectroscopy

IETS is a vibrational spectroscopic method in which vibrational modes are detected by their influence on electronic conduction in a tunnel junction.[53] Most tunneling of electrons through a barrier occurs elastically, therefore the electrons traverse the junction at a constant energy. Inelastic tunneling occurs when an electron interacts with a vibrational mode or phonon during the tunneling process and energy transfer takes place. This conduction process can only occur when the electron energy is greater than the vibrational energy. It can be detected as a change in slope in the current voltage characteristics which corresponds to a step in the conductance characteristics or a peak in the derivative of conductance. Experimentally this effect is measured directly by applying a dc bias and a small ac probe signal. The second harmonic of the ac signal is measured as a function of dc bias and vibronic modes appear as peaks in this spectrum. The voltage at which these peaks occur corresponds to the vibrational mode energy which can easily be expressed as a wavenumber. Due to thermal broadening considerations, this measurement must be performed near liquid helium temperatures, which in turn requires the use of degenerately doped silicon substrates. This technique has the advantage that it offers a direct measurement of molecular vibronic structure in a transport device architecture. The fabrication and inelastic electron tunneling spectroscopy (IETS) characterization of gold/molecule/*p*+ silicon structures for several molecular species has been reported recently, demonstrating that this technique can resolve molecular vibronic features for aliphatic and substituted aromatic molecules.[31] The IETS spectra from N-benz are shown in Fig. 14 along with the corresponding pb-RAIRS data for comparison. Peak assignments were made based on comparison of the spectra with infrared and Raman spectra from the literature. The peak marked " *" could not be unambiguously assigned. The observation of peaks associated with the molecular headgroup (NO_2) and ring modes such as the C–C stretch (νCC) confirm the presence of the molecular layer. The Si–H stretch mode indicates the contribution of the Si contact in this measurement.

C. Comparison of *in situ* spectroscopic measurements

IETS and pb-RAIRS of gold/molecule/silicon structures should be considered simultaneously and compared to offer the most complete description of the system possible. As illustrated by the infrared and tunneling spectra of a N-benz molecular layer (Fig. 14), the vibrational spectra obtained by the two methods exhibit similarities and differences which can be considered in some detail. For the IR spectrum, modes related to the NO_2 headgroup and silicon oxide are very prominent. The peaks are quite sharp and well defined. There are no clear features in the expected spectral regions for vibrations related to the carbon in the molecular layer or to silicon-hydrogen species. The IETS, on the other hand, has prominent modes related to the benzene ring and Si–H stretches, weak modes related to the NO_2 headgroup, and no detectable silicon oxide signal. The IETS peaks are relatively broad compared with the peaks in the IR spectrum. These similarities and differences can be understood by considering differences between the selection rules for the two experiments. IR spectroscopy is sensitive to strongly dipolar bonds, therefore the oxygen-containing modes are well resolved. Since it is an electronic measurement, IETS is sensitive to vibronic or coupled electronic-vibrational modes. Although the selection rules for such coupled modes are not well characterized, there is some evidence that vibrational modes which interact strongly with the contacts are most readily resolved.[54] The observation that Si–H and benzene modes are most prominent in the IETS is consistent with this description of the selection rules. These observations illustrate the value of applying multiple characterization techniques to the same system and illustrate the need to develop additional methods to characterize the structural and chemical compositions of metallized molecular layers.

The difference in peak widths between IETS and pb-RAIRS is due to the different probes and the physics by which they interact with the vibrational modes. In pb-RAIRS, light is used as a probe, therefore the intrinsic linewidth of the measurement is very small and the peak width closely reflects the actual distribution of vibrational energies. In IETS, an ac current is used to probe the molecular vibrations. In this case, there are broadenings associated with the thermal distribution of electrons and the ac modulation amplitude in addition to the intrinsic linewidth of the measurement.[53] Collectively, these effects are responsible for the broader observed peak widths.

V. CONCLUSION

A series of substituted aryl-diazonium salts have been grafted to hydrogen-terminated ⟨111⟩-orientation silicon surfaces and characterized using a variety of techniques. Collectively, these measurements suggest that Br-, OCH_3-, and $N(C_2H_5)_2$-substituted molecules form relatively ideal, approximately single monolayer films. These samples show a slight amount of substrate oxidation and some hydrocarbon contamination on the sample surfaces. NO_2-substituted mo-

lecular layers exhibit relatively less-ideal behavior with a higher degree of substrate oxidation and some evidence of NH_x headgroup formation. Characterization of metallized molecular layers shows that soft evaporation of gold yields relatively unaltered vibrational spectra, whereas copper significantly degrades the molecular signature. The simultaneous analysis of infrared and tunneling spectroscopies offers complimentary evidence suggesting that N-benz layers are not significantly perturbed by soft evaporation of gold.

ACKNOWLEDGMENTS

The authors would like to thank Dmitri Zemlyanov for performing XPS measurements. The authors thank Christina A. Hacker, Nadine Gergell-Hackett, Curt A. Richter, and Lee J. Richter for assistance with pb-RAIRS measurements, Wenyong Wang for performing IETS measurements, and Chad Risko for DFT calculations. The authors would like to acknowledge Mark Hersam and Mark Ratner for helpful discussions. This work is supported by NSF under Grant No. ECS-0506802. A. Scott is supported by a NSF Graduate Research Fellowship.

[1]D. K. Aswal, S. Lenfant, D. Guerin, J. V. Yakhmi, and D. Vuillaume, Anal. Chim. Acta **568**, 84 (2006).
[2]P. Allongue, C. H. de Villeneuve, and J. Pinson, Electrochim. Acta **45**, 3241 (2000).
[3]A. Bansal and N. S. Lewis, J. Phys. Chem. B **102**, 1067 (1998).
[4]A. Faucheux, A. C. Gouget-Laemmel, P. Allongue, C. H. de Villeneuve, F. Ozanam, and J.-N. Chazalviel, Langmuir **23**, 1326 (2007).
[5]J. M. Buriak, Chem. Commun. (Cambridge) **1999**, 1051.
[6]J. M. Buriak, Chem. Rev. (Washington, D.C.) **102**, 1272 (2002).
[7]M. R. Linford, P. Fenter, P. M. Eisenberger, and C. E. D. Chidsey, J. Am. Chem. Soc. **117**, 3145 (1995).
[8]R. Boukherroub, S. Morin, D. D. M. Wayner, F. Bensebaa, G. I. Sproule, J. M. Baribeau, and D. J. Lockwood, Chem. Mater. **13**, 2002 (2001).
[9]A. Bansal, X. Li, I. Lauermann, N. S. Lewis, S. I. Yi, and W. H. Weinberg, J. Am. Chem. Soc. **118**, 7225 (1996).
[10]R. Boukherroub, S. Morin, F. Bensebaa, and D. D. M. Wayner, Langmuir **15**, 3831 (1999).
[11]S. Fellah, A. Teyssot, F. Ozanam, J.-N. Chazalviel, J. Vegneron, and A. Etcheberry, Langmuir **18**, 5851 (2002).
[12]R. L. Cicero, M. R. Linford, and C. E. D. Chidsey, Langmuir **16**, 5688 (2000).
[13]J. M. Tour, L. J. II, D. L. Pearson, J. J. S. Lamba, T. P. Bugin, G. M. Whitesides, D. L. Allara, A. N. Parkh, and S. V. Atre, J. Am. Chem. Soc. **117**, 9529 (1995).
[14]C. H. de Villeneuve, J. Pinson, M. C. Bernard, and P. Allongue, J. Phys. Chem. B **101**, 2415 (1997).
[15]D. V. Kosynkin and J. M. Tour, Org. Lett. **3**, 993 (2001).
[16]M. P. Stewart, F. Maya, D. V. Kosynkin, S. M. Dirk, J. J. Stapleton, C. L. McGuiness, D. L. Allara, and J. M. Tour, J. Am. Chem. Soc. **126**, 370 (2004).
[17]P. Allongue, C. H. de Villeneuve, J. Pinson, F. Ozanam, J. N. Chazalviel, and X. Wallart, Electrochim. Acta **43**, 2791 (1998).
[18]R. Basu, C. R. Kinser, J. D. Tovar, and M. C. Hersam, Chem. Phys. **326**, 144 (2006).
[19]D. Pandey, D. Y. Zemlyanov, K. Bevan, R. G. Reifenberger, S. M. Dirk, S. W. Howell, and D. R. Wheeler, Langmuir **23**, 4700 (2007).
[20]C. L. McGuiness, D. Blasini, J. P. Masejewski, S. Uppili, O. M. Cabarcos, D. Smilgies, and D. L. Allara, ACS Nano **1**, 30 (2007).
[21]P. Allongue, C. H. de Villeneuve, G. Cherouvrier, R. Cortes, and M.-C. Bernard, J. Electroanal. Chem. **550–551**, 161 (2003).
[22]F. Anariba, S. H. DuVall, and R. L. McCreery, Anal. Chem. **75**, 3837 (2003).
[23]M. Gensch, K. Roodenko, K. Hinrichs, R. Hunger, A. G. Güell, A. Merson, U. Schade, Y. Shapira, T. Dittrich, J. Rappich, and N. Esser, J. Vac. Sci. Technol. B **23**, 1838 (2005).
[24]K. Roodenko, J. Rappich, M. Gensch, N. Esser, and K. Hinrichs, Appl. Phys. A: Mater. Sci. Process. **90**, 175 (2008).
[25]A. Scott, D. B. Janes, C. Risko, and M. A. Ratner, Appl. Phys. Lett. **91**, 033508 (2007).
[26]A. Vilan, A. Shanzer, and D. Cahen, Nature (London) **404**, 166 (2000).
[27]H. Haick, M. Ambrico, T. Ligonzo, R. T. Tung, and D. Cahen, J. Am. Chem. Soc. **128**, 6854 (2006).
[28]H. Haick, O. Niitsoo, J. Ghabboun, and D. Cahen, J. Phys. Chem. C **111**, 2318 (2007).
[29]A. V. Walker, T. B. Tighe, J. Stapleton, B. C. Haynie, S. Uppili, D. L. Allara, and N. Winograd, Appl. Phys. Lett. **84**, 4008 (2004).
[30]G. Nagy and A. V. Walker, J. Phys. Chem. B **110**, 12543 (2006).
[31]W. Wang, A. Scott, N. Gergel-Hackett, C. Hacker, D. B. Janes, and C. Richter, Nano Lett. **8**, 919 (2008).
[32]C. A. Richter, C. A. Hacker, L. J. Richter, O. A. Kirillov, J. S. Suehle, and E. M. Vogel, Solid-State Electron. **50**, 1088 (2006).
[33]G. S. Higashi, Y. J. Chabal, G. W. Trucks, and K. Raghavachari, Appl. Phys. Lett. **56**, 656 (1990).
[34]P. Jakob and Y. J. Chabal, J. Chem. Phys. **95**, 2897 (1991).
[35]C. P. Wade and C. E. D. Chidsey, Appl. Phys. Lett. **71**, 1679 (1997).
[36]M. R. Houston and R. Maboudian, J. Appl. Phys. **78**, 3801 (1995).
[37]P. Hartig, J. Rappich, and T. Dittrich, Appl. Phys. Lett. **80**, 67 (2002).
[38]R. M. Metzger, T. Xu, and I. R. Peterson, J. Phys. Chem. B **105**, 7280 (2001).
[39]S. Lodha and D. B. Janes, Appl. Phys. Lett. **85**, 2809 (2004).
[40]N. Fairley, CASAXPS software version 2.3.12.
[41]NIST XPS database, URL http://srdata.nist.gov/xps.
[42]C. S. Fadley, R. J. Baird, W. Siekhaus, T. Novakov, and S. A. L. Bergstrom, J. Electron Spectrosc. Relat. Phenom. **4**, 93 (1974).
[43]P. J. Cumpson and M. P. Seah, Surf. Interface Anal. **25**, 430 (1997).
[44]M. Suzuki, H. Ando, Y. Higashi, H. Takenaka, H. Shimada, N. Matsubayashi, M. Imamura, S. Kurosawa, S. Tanuma, and C. J. Powell, Surf. Interface Anal. **29**, 330 (2000).
[45]R. Larsson and B. Folkesson, Chem. Scr. **9**, 148 (1976).
[46]J. Sharma, W. L. Garrett, F. J. Owens, and V. L. Vogel, J. Phys. Chem. **86**, 1657 (1982).
[47]D. Varsanyi,*Assignments for Vibrational Spectra of Seven Hundred Benzene Derivatives* (Wiley, New York, 1973).
[48]R. M. Silverstein and F. X. Webster, *Spectrometric Identification of Organic Compounds* (Wiley, New York, 1998).
[49]M. Avram and G. D. Mateescu, *Infrared Spectroscopy: Applications in Organic Chemistry* (Wiley, New York, 1972).
[50]A. V. Walker, T. B. Tighe, O. Cabarcos, M. D. Reinard, S. Uppili, B. C. Haynie, N. Winograd, and D. L. Allara, J. Am. Chem. Soc. **126**, 3954 (2004).
[51]A. Scott, C. A. Hacker, and D. B. Janes, J. Phys. Chem. C **112**, 14021 (2008).
[52]C. A. Richter, C. A. Hacker, and L. J. Richter, J. Phys. Chem. B **109**, 21836 (2005).
[53]W. Wang, T. Lee, I. Kretzschmar, and M. A. Reed, Nano Lett. **4**, 643 (2004).
[54]J. M. Beebe, H. J. Moore, T. R. Lee, and J. G. Kushmerick, Nano Lett. **7**, 1364 (2007).